Journal of Materials Chemistry C

PAPER

View Article Online
View Journal | View Issue

Cite this: J. Mater. Chem. C, 2015, 3, 2399

Aggregation-induced chirality, circularly polarized luminescence, and helical self-assembly of a leucine-containing AIE luminogen

Hongkun Li,†[ac] Juan Cheng,[d] Haiqin Deng,[bc] Engui Zhao,[bc] Bo Shen,[c] Jacky W. Y. Lam,[bc] Kam Sing Wong,[d] Hongkai Wu,[c] Bing Shi Li*[a] and Ben Zhong Tang*[bc]

Received 28th November 2014
Accepted 12th January 2015

DOI: 10.1039/c4tc02726d

www.rsc.org/MaterialsC

Self-assembling of luminescent molecules into one-dimensional nanostructures is of particular interest in fabricating nanoscale electronic and photonic devices. Herein, we report the rational design and synthesis of a chiral fluorescent tetraphenylethylene derivative containing L-leucine methyl ester moiety (**TPE-Leu**). In solution, **TPE-Leu** is non-emissive and CD silent, but becomes highly emissive and CD active upon aggregation, exhibiting aggregation-induced emission (AIE) and chirality (AIC). Upon evaporation of its solution, **TPE-Leu** readily self-assembles into helical fluorescent micro/nanofibers, which show circularly polarized luminescence (CPL) and have the CPL dissymmetry factors in the range of 0.02–0.07. This molecular design combines the AIE effect, chirality, and self-assembling capability together, and is highly efficient in constructing novel functional micro/nanomaterials with well-defined structures and enhanced emission.

Introduction

Fabrication of functional architectures by bottom-up molecular assembly is an important approach for the design of micro and nano devices.[1] By deliberately designing the cooperative molecular building blocks, a controllable self-assembly can be realized to construct desirable architectures with novel functions. π-conjugated luminescent molecules are ideal building blocks for the molecular assembly due to their unique optoelectronic properties and have potential applications in optoelectronic devices and biological sensors.[2] Compared with "conventional" organic fluorophores, the luminogens with AIE characteristics are newly emerging "stars".[3] AIE molecules, as represented by silole, tetraphenylethylene (TPE), triphenylethene, distyrylanthracene, and their derivatives, are non-emissive in solution, but become highly luminescent in the condensed state.[4] This unique AIE property overcomes the notorious aggregation-caused quenching (ACQ) effect that conventional fluorescent molecules normally suffer in their aggregated or solid state.[5]

Precise self-assembling of AIE molecules into desired architectures, such as nanoparticles, nanorods and nanofibers, is still a challenging task.[6] Among the various morphological structures, one-dimensional (1D) fluorescent nanorods and nanofibers with AIE properties are of considerable interest because they are in high demand in optoelectronic devices for transferring current and optical signals. Zhang and coworkers reported the controllable self-assembly of di(*p*-methoxyphenyl)-dibenzofulvene into microrods with different emission colors and efficiencies in the presence of different concentrations of cetyltrimethylammonium bromide.[7] Šket synthesized a BF_2 complex with AIE property, which can form the fluorescent microfibers through the sublimation process.[8] Huang *et al.* fabricated the luminescent 1D nanorods by the self-assembly of two four-armed TPE derivatives containing electron-rich and electron-deficient groups driven by charge-transfer interactions.[9] Zhu and Zhao prepared an AIE-active dicyanomethylene-4*H*-pyran (DCM) derivative with high red-emission, which can self-assemble into 1D micro/nanowires.[10] Our groups constructed the efficient fluorescent microfibers and nanorods by the self-assembling of TPE-based luminogens.[11] Recently, we have been endowing the fluorescent nanofibers with chiral properties, by the introduction of amino acid attachments to the AIE scaffold.[12] We have successfully prepared valine-containing silole and TPE, which self-assembled into helical nanofibers with enhanced emission and circularly polarized

[a]*Key Laboratory of New Lithium-Ion Battery and Mesoporous Material, Department of Chemistry and Chemical Engineering, Shenzhen University, Shenzhen 518060, China. E-mail: phbingsl@google.com; Fax: +86-755-26536141; Tel: +86-755-26558094*

[b]*The Hong Kong University of Science & Technology (HKUST) – Shenzhen Research Institute, No. 9 Yuexing 1st RD, South Area, Hi-tech Park, Nanshan, Shenzhen 518057, China. E-mail: tangbenz@ust.hk*

[c]*Department of Chemistry, Institute for Advanced Study, Institute of Molecular Functional Materials, State Key Laboratory of Molecular Neuroscience, HKUST, Clear Water Bay, Kowloon, Hong Kong, China*

[d]*Department of Physics, HKUST, Clear Water Bay, Kowloon, Hong Kong, China*

† Current address: College of Chemistry, Chemical Engineering and Materials Science, Soochow University, Suzhou 215123, China.

luminescence (CPL) properties. The optical properties and the self-assembling behaviors are determined both by the AIE scaffold and amino acid attachments. Elucidating the cooperative effects of different combinations of the building blocks is necessary for better understanding the underlying principles and improving the rational molecular design.

Our previous work showed that introducing L-leucine methyl ester units into the pendants of polyphenylacetylene can efficiently induce the polymer to have helical conformation. The helical conformation was further amplified as helical nanofibers on the higher order construction of the polymer.[13] Inspired by this idea, we design a TPE molecule with a L-leucine methyl ester attachment (**TPE-Leu**). This compound is non-luminescent and circular dichroism (CD) silent in solution. Upon aggregate formation, it emits intensely and also gives strong CD signals, showing the typical AIE and AIC properties. **TPE-Leu** self-assembles into helical micro/nanofibers, which are circularly polarized luminescent and exhibit large CPL dissymmetry factors.

Results and discussion

Following the synthesis route shown in Scheme 1, **TPE-Leu** was prepared as a white solid powder with a yield of 81%. The product was carefully purified and characterized by NMR, high-resolution mass spectrometry and elemental analysis, from which satisfactory results were obtained (see Experimental section for details).

The UV spectra of **TPE-Leu** in 1,2-dichloroethane (DCE), DCE–hexane suspension and cast film given in Fig. 1A, show absorption peaks located at the wavelength of about 315 nm, which corresponds to the absorption of the TPE unit. CD spectra are also captured to check whether the chirality of the amino acid attachment has been transferred to the TPE scaffold. As shown in Fig. 1B, no CD signal is observed in DCE solution of **TPE-Leu**, which may be caused by the random orientation of the chromophores in solution.[14] However, when hexane, the poor solvent of **TPE-Leu**, is added, it displays two CD peaks at the wavelength of 258 and 295 nm in DCE–hexane suspension (1/9, v/v), respectively. These two peaks correspond to the absorption of the leucine-containing triazolylphenyl group, suggesting the occurrence of an AIC effect.[15] We then studied the optical activity of **TPE-Leu** in its cast film, which was formed by natural evaporation of its DCE solution on a quartz substrate. The film does not show a conventional "film" appearance, but actually consists of a large number of fibers. It exhibits strong cotton effects and a new peak at the wavelength of ~328 nm as well. Because the leucine-containing unit (2) is

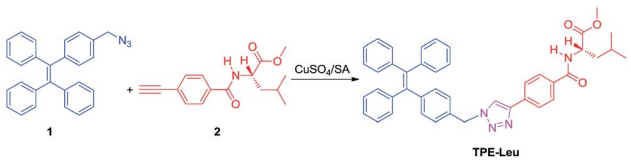

Scheme 1 Synthesis route to **TPE-Leu**. SA = sodium ascorbate.

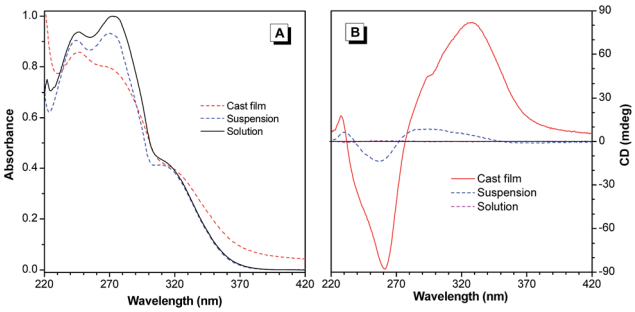

Fig. 1 (A) UV absorption spectra of **TPE-Leu** in 1,2-dichloroethane (DCE) solution and DCE–hexane (1/9, v/v) suspension with concentration of 3×10^{-5} M, and cast film prepared by natural evaporation of its DCE solution. (B) CD spectra of **TPE-Leu** in DCE solution and DCE–hexane (1/9, v/v) suspension with concentration of 10^{-4} M, and cast film prepared by natural evaporation of its DCE solution of 0.66 mg mL^{-1}.

CD-silent at the wavelengths longer than 300 nm,[16] the new peak must stem from the absorption of the TPE moiety. It indicates that chirality has been successfully transferred from the chiral amino acid attachments to the TPE units, giving rise to the formation of a preferred-handed helical conformation in the aggregate state.

We then studied the fluorescence of **TPE-Leu** in THF–water mixtures with different water fractions (f_w). As shown in Fig. 2A, the photoluminescence (PL) curves of **TPE-Leu** in THF and THF–water mixtures with f_w lower than 70% are almost flat lines parallel to the abscissa. The PL intensities of **TPE-Leu** are enhanced significantly when f_w is higher than 70%. The highest intensity was reached at the f_w of 90%, which is 460-fold higher than that in THF solution (Fig. 2B). Because water is a poor solvent for **TPE-Leu**, the addition of water to the THF solution likely induces the formation of aggregates. At high water fraction in the mixture, a majority of **TPE-Leu** will aggregate, which blocks the non-radiative energy transference and turns on the fluorescence of the molecules.[4f] Therefore, **TPE-Leu** still keeps the AIE property with an introduction of leucine attachments.

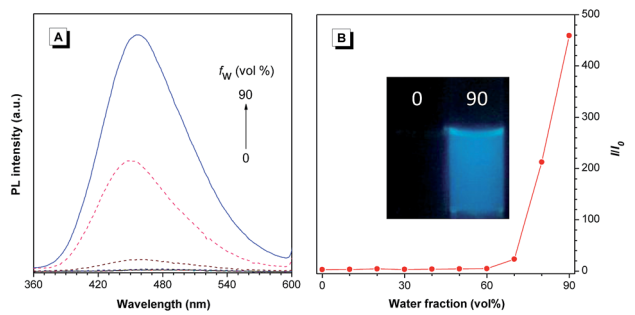

Fig. 2 (A) PL spectra of **TPE-Leu** in THF–water mixtures with different water fraction (f_w). Concentration: 20 μM; λ_{ex}: 315 nm. (B) Plot of relative emission peak intensity (I/I_0) at 456 nm *versus* f_w of the THF–water mixture, where I = emission intensity and I_0 = emission intensity in THF solution. Inset: images of **TPE-Leu** in THF–water mixtures with f_w of 0 and 90 taken under a hand-held UV lamp.

Generally, molecules exhibit CPL property when either their luminophores or an ensemble of luminophores is chiral. As we know, CPL is the emission analog of CD, which can provide the specific information about the chirality of the fluorophores in the excited state. The CPL activity is commonly evaluated by the emission dissymmetry factor (g_{em}), defined as $g_{em} = 2(I_L - I_R)/(I_L + I_R)$, where I_L and I_R are the intensities of left- and right-handed emissions, respectively. CPL-active organic materials have attracted much interest in recent years for their potential applications in bio/chemosensors and optoelectronic devices, such as CPL lasers, optical storage and processing systems.[17] It is reported that most of pure organic small molecules display the g_{em} values in the range of 10^{-5}–10^{-2} in their solutions.[18] However, in solid state, their CPL performance usually becomes weakened due to the ACQ effect. Furthermore, the structural diversity of the chiral organic fluorophores is limited, most of which are helicene and 1,1-binaphthyl derivatives.[18,19] Development of new organic materials with efficient CPL performance in solid state is thus in great demand.

Considering that **TPE-Leu** is highly emissive and CD-active in the solid state, it is anticipated to possess CPL properties. We then studied the CPL behavior of the cast film of **TPE-Leu** using a home-built CPL measurement system.[15] As can be seen from Fig. 3, the solid film of **TPE-Leu** exhibits a positive signal in the CPL spectrum. The g_{em} values are in the range from 0.02 to 0.07 in the detected spectral window of 360–600 nm. At the wavelength of maximum emission, the g_{em} value of **TPE-Leu** is about 0.05, which is higher than that of valine-containing TPE reported in our previous work.[12b]

In term of its simple synthesis, emission efficiency and dissymmetry factor in solid state, **TPE-Leu** is thus a promising candidate for fabricating advanced electronic CPL devices for bio-sensing and optoelectronic applications.

The cast film on a quartz plate prepared by the evaporation of the DCE solution of **TPE-Leu** exhibits fiber-like morphology, implying that **TPE-Leu** tends to self-assemble to form regular structures rather than forming random aggregates. The self-assembling behaviors of **TPE-Leu** were then explored with a variety of microscopy imaging techniques. We then checked the self-assemblies of **TPE-Leu** induced by the addition of poor solvents of hexane to its DCE solutions. Upon the evaporation of its DCE–hexane (1/9, v/v) mixture, **TPE-Leu** assembled into helical fibers and helical ribbons, as shown in the SEM images in Fig. 4A and B. The helical fibers/ribbons are predominantly left-handed, which corresponds well with the CD and CPL spectra. In contrast to the small fraction of helical ribbons, the helical fibers are dominant and thin fibers further braid together to form thicker ones. Due to their hierarchical assemblies, the helical fibers have a broad width distribution from ~15 to 350 nm and also a wide distribution of helical pitch up to a maximum of 920 nm. Along with the helical fibers and helical ribbons, there are also combined structures exhibiting both the morphology of helical ribbons and fibers, as clearly shown in Fig. 4B. The ribbon in the upper right corner labeled with arrows has several helical knots along its contour, which are not evenly located along the ribbon due to their varying extents of helical wrapping and diverse tilting directions. Similar kind of morphology is also found for the ribbons labeled in the left part of the image. These combined structures of helical ribbons and helical fibers suggest that they are the intermediates of the morphological transition from helical ribbons to helical fibers and the latter are likely formed by the wrapping up of the former. In addition to SEM, the TEM image of **TPE-Leu** in Fig. 4C also confirms the existence of helical fibers and helical ribbons with preferred left-handedness. The fluorescence microscope image of **TPE-Leu** further shows that these helical fibers are several millimeters long and they emit intensive blue fluorescence, as shown in Fig. 4D.

TPE-Leu exhibited a similar assembling manner to what has been reported for amino acid-containing amphiphilic molecules, namely they all form helical fibers or ribbons.[20] The helical assemblies are directed by the chirality of the amino acid attachments of the molecules, which exert asymmetric force fields to the TPE scaffold to induce it to twist. The organization likely starts from the formation of chiral layers or ribbons, followed by another organization level that chiral layers or ribbons further twist or wrap up to form helical fibers or tubes.

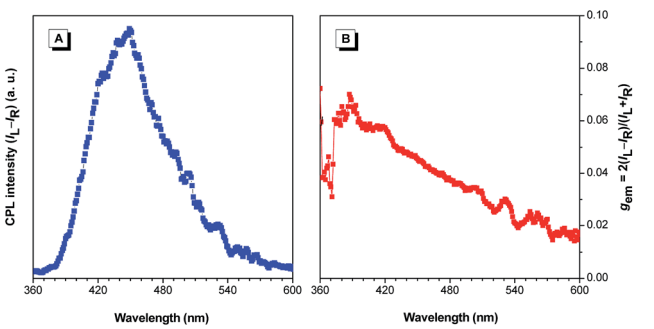

Fig. 3 Plots of (A) CPL and (B) CPL dissymmetry factor g_{em} *versus* wavelength of cast film of **TPE-Leu** prepared by the evaporation of its solution, λ_{ex}: 325 nm.

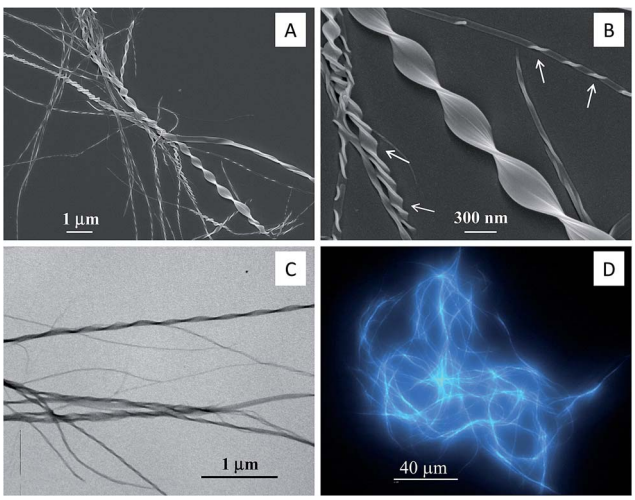

Fig. 4 (A and B) SEM, (C) TEM and (D) fluorescence microscopy images of the aggregates of **TPE-Leu** formed in DCE–hexane (1/9, v/v) mixture, concentration: 10^{-4} M.

Intermolecular hydrogen bonds of the amino acid attachments and π–π stacking of TPE scaffold cooperatively stabilize the twisting arrangements of the molecules. The chiral amino acid attachments are critical in determining the assembling behavior and related optical properties, for they not only guide the packing of the molecules in the chiral molecular layers or ribbons, but also direct the tilting directions of the precursors. Bulkier chiral attachments are generally more efficient to exert asymmetric force field to the TPE scaffold and induce more significant helical twists in the chiral molecular packing. The twist will be further amplified on the next organization level as the construction of helical ribbons or fibers. As a consequence of the contribution of the bulky amino acid attachments, intensive CD absorption is expected. The CPL property, which is the chirality of the luminogens, is determined both by the helicity and luminescence of the molecules. An excellent CPL property of a molecule comes from an optimized balanced effect of high CD absorption and luminescence. The CPL property of **TPE-Leu** is higher than that of valine-containing TPE reported in our previous work, suggesting that leucine attachment induces a better cooperative CPL property. The g_{em} value of the resultant **TPE-Leu** fibers is also high as compared with the reported pure organic luminescent molecules,[18,19] suggesting that leucine attachment is an ideal candidate that guides the resultant molecule to come up with both regular helical assemblies and an excellent CPL performance.

Conclusions

In summary, novel luminescent helical fibers are constructed by the assembling of L-leucine methyl ester-modified TPE. The deliberately designed **TPE-Leu** molecule inherits the typical AIE characteristic from TPE unit, chirality from the amino acid attachments and a remarkable CPL performance as a cooperative contribution of both groups. These novel properties make these kind of fibers promising candidates for optoelectronics and biological applications. This rational bottom-up nanofabrication by the non-covalent interactions of molecules is an efficient way to construct novel functional micro/nanomaterials with well-defined structures and enhanced emission. It provides an important shortcut for the combination of AIE effect and chirality with the self-assembled structures. The cooperative effect of chiral attachments and AIE scaffold on the optical properties of molecule is pivotal for a maximum output of the performance of the assembled structures. Deciphering the bulkiness effect and the involved non-covalent interactions help to better understand the underlying mechanism of the hierarchical assembling process and its resultant optical properties. It is still a challenging task both in the molecular design and synthesis, and is worth exploring further.

Experimental section

General information

Tetrahydrofuran (THF) was distilled from sodium benzophenone ketyl in an atmosphere of nitrogen just prior to use. L-Ascorbic acid, sodium bicarbonate, copper(II) sulfate, and other chemicals and solvents were all purchased from Aldrich and used as received without further purification.

The ^{1}H and ^{13}C NMR spectra were recorded on a Bruker ARX 400 NMR spectrometer in $CDCl_3$ using tetramethylsilane (TMS; $\delta = 0$) as internal reference. High-resolution mass spectra (HRMS) were recorded on a GCT Premier CAB 048 mass spectrometer in an electron-ionization or a MALDI-TOF mode. UV absorption spectra were measured on a Milton Ray Spectronic 3000 array spectrophotometer. Photoluminescence (PL) spectra were recorded on a PerkinElmer LS 55 spectrofluorometer. Morphological structures of the aggregates were examined by JEOL 2010 transmission electron microscope (TEM) at accelerating voltages of 200 kV and JEOL-6700F scanning electron microscope (SEM) 5 kV, respectively. CD spectra were taken on a JASCO J-810 spectropolarimeter in a 1 mm quartz cuvette using a step resolution of 0.1 nm, a scan speed of 100 nm min^{-1}, a sensitivity of 0.1 nm, and a response time of 0.5 s. Circular photoluminescence spectra (CPL) were recorded on a home-made CPL spectroscopy system.[15] A 325 nm He–Cd laser was used as an excitation light source. The retardation of the emitted light from the sample is modulated by a photo-elastic modulator (PEM; Hinds PEM-90, 50 kHz) and detected by the photomultiplier tube (PMT) after passing through the linear polarizer oriented at 45° to the PEM optical axis. The combination of PEM and the linear polarizer provides modulation of the circularly polarized part of the total emission. The DC component of the PMT output is measured by a digital multimeter (Thurlby 1905a), where the total intensity of left (I_L) and right (I_R) of circularly polarized emitted light can be obtained (*i.e.*, $I_L + I_R$). On the other hand, the AC component is amplified by a pre-amplifier (Stanford Research Systems, SR560) and analyzed by a lock-in amplifier (Stanford Research Systems, SR510), so that the alternating signals with regard to emitted left and right polarization is detected (*i.e.*, $I_L - I_R$). Then, the CPL dissymmetry factor, $g_{em} = 2(I_L - I_R)/(I_L + I_R)$, was derived from the ratio of AC signal to the DC signal.

Sample preparation for PL measurement

A stock THF solution of 2×10^{-4} M **TPE-Leu** was first prepared. Aliquots of the stock solution were transferred to 10 mL volumetric flasks. After appropriate amounts of THF were added, distilled water was added dropwise with vigorous stirring to yield 2×10^{-5} M solutions with different water fractions (0–90 vol%). The PL measurements of the resulting solutions were then conducted immediately.

Sample preparation for SEM and TEM measurements

A stock DCE solution of **TPE-Leu** (1×10^{-3} M) was first prepared. The stock solution was then transferred to 5 mL glass vial and diluted to the suspension with a final concentration of 1×10^{-4} M by adding hexane dropwise with vigorous stirring. 4 μL of this suspension was immediately dropped onto the surface of silicon wafer and carbon-coated copper grid. After evaporation of the solvent under ambient conditions, the samples were characterized by SEM and TEM, respectively.

Synthesis

1-[4-(Azidomethyl)phenyl]-1,2,2-triphenylethene (**1**) and 4-ethynylbenzoyl-L-leucine methyl ester (**2**) were prepared according to our previous papers.[16,21]

Synthesis of 4-{1-[4-(1,2,2-triphenylvinyl)benzyl]triazoyl} benzoyl-L-leucine methyl ester (TPE-Leu). Into a 100 mL two necked round-bottom flask, were added 0.426 g (1.1 mmol) of 1-[4-(azidomethyl)phenyl]-1,2,2-triphenylethene (**1**) and 0.273 g (1.0 mmol) of 4-ethynylbenzoyl-L-leucine methyl ester (**2**) in 45 mL of water–THF–ethanol (1/1/1, v/v/v) under nitrogen. 1.25 mL of freshly prepared 1 M aqueous solution of sodium ascorbate was added followed by 24 mg (0.15 mmol) of copper sulfate in 0.5 mL of water. The reaction mixture was stirred at 70 °C overnight. After cooling to room temperature, 50 mL of water was added and the resultant solution was extracted with DCM. The combined organic layer was washed with brine, ethylenediaminetetraacetic acid disodium salt solution and water, and then dried over Na_2SO_4 overnight. After filtration and solvent evaporation, the crude product was purified by a silica gel column using DCM–ethyl acetate mixture (10 : 1, v/v) as eluent. A white solid of TPE-Leu was obtained with a yield of 81%. ^{1}H NMR (400 MHz, $CDCl_3$), δ (TMS, ppm): 7.87 (m, 4H), 7.65 (s, 1H), 7.09 (m, 9H), 7.05 (m, 4H), 7.01 (m, 6H), 6.53 (d, 1H), 5.48 (s, 2H), 4.88–4.85 (m, 1H), 3.78 (s, 3H), 1.80–1.72 (m, 2H), 1.70–1.66 (m, 1H), 1.01–0.98 (m, 6H). ^{13}C NMR (100 MHz, $CDCl_3$), δ (TMS, ppm): 173.8, 166.7, 147.1, 144.7, 143.5, 143.4, 143.3, 141.9, 140.1, 134.0, 133.3, 132.3, 132.2, 131.3, 127.8, 127.6, 126.8, 125.7, 120.3, 54.2, 52.5, 51.3, 42.0, 25.1, 23.0, 22.0. HRMS (MALDI-TOF), m/z 660.3118, (M^+, calcd 660.3100). Anal. calcd for $C_{43}H_{40}N_4O_3$: C, 78.16; H, 6.10, N, 8.48. Found: C, 78.22; H, 6.10, N, 8.54.

Acknowledgements

This work was partially supported by the National Natural Science foundation of China (21104046 and 21404077), the Outstanding Youth foundation of Shenzhen (JC201005250038A, JCYJ20140509172609153), the National Basic Research Program of China (973 program, 2013CB834701), the Research Grants Council of Hong Kong (604711, 604913 and N_HKUST620/11) and the University Grants Committee of Hong Kong (AoE/P-03/08).

Notes and references

1 (*a*) J. M. Lehn, *Science*, 2002, **295**, 2400; (*b*) G. M. Whitesides and B. Grzybowski, *Science*, 2002, **295**, 2418.
2 (*a*) Y. Li, T. Liu, H. Liu, M. Z. Tian and Y. Li, *Acc. Chem. Res.*, 2014, **47**, 1186; (*b*) L. Magginia and D. Bonifazi, *Chem. Soc. Rev.*, 2012, **41**, 211; (*c*) A. Kaeser and A. P. H. J. Schenning, *Adv. Mater.*, 2010, **22**, 2985; (*d*) L. Zang, Y. Che and J. S. Moore, *Acc. Chem. Res.*, 2008, **41**, 1596.
3 J. Luo, Z. Xie, J. W. Y. Lam, L. Cheng, H. Chen, C. Qiu, H. S. Kwok, X. Zhan, Y. Liu, D. Zhu and B. Z. Tang, *Chem. Commun.*, 2001, 1740.
4 (*a*) Y. Hong, J. W. Y. Lam and B. Z. Tang, *Chem. Commun.*, 2009, 4332; (*b*) Y. Hong, J. W. Y. Lam and B. Z. Tang, *Chem. Soc. Rev.*, 2011, **40**, 5361; (*c*) Z. Zhao, J. W. Y. Lam and B. Z. Tang, *J. Mater. Chem.*, 2012, **22**, 23726; (*d*) Z. G. Chi, X. Q. Zhang, B. J. Xu, X. Zhou, C. P. Ma, Y. Zhang, S. W. Liu and J. R. Xu, *Chem. Soc. Rev.*, 2012, **41**, 3878; (*e*) J. B. Zhang, B. Xu, J. L. Chen, S. Q. Ma, Y. J. Dong, L. J. Wang, B. Li, L. Ye and W. J. Tian, *Adv. Mater.*, 2014, **26**, 739; (*f*) J. Mei, Y. Hong, J. W. Y. Lam, A. Qin, Y. Tang and B. Z. Tang, *Adv. Mater.*, 2014, **26**, 5429.
5 J. B. Birks, *Photophysics of Aromatic Molecules*, Wiley, New York, 1970.
6 (*a*) Z. Zhao, J. W. Y. Lam and B. Z. Tang, *Soft Matter*, 2013, **9**, 4564; (*b*) B. K. An, J. Gierschner and S. Y. Park, *Acc. Chem. Res.*, 2012, **45**, 544; (*c*) C. Zhang, S. Jin, S. Li, X. Xue, J. Liu, Y. Huang, Y. Jiang, W.-Q. Chen, G. Zou and X.-J. Liang, *ACS Appl. Mater. Interfaces*, 2014, **6**, 5212; (*d*) H. T. Feng, S. Song, Y. C. Chen, C. H. Shen and Y. S. Zheng, *J. Mater. Chem. C*, 2014, **2**, 2353; (*e*) C. Niu, L. Zhao, T. Fang, X. Deng, H. Ma, J. Zhang, N. Na, J. Han and J. Ouyang, *Langmuir*, 2014, **30**, 2351; (*f*) J. Li, Y. Li, C. Y. K. Chan, R. T. K. Kwok, H. Li, P. Zrazhevskiy, X. Gao, J. Z. Sun, A. Qin and B. Z. Tang, *Angew. Chem., Int. Ed.*, 2014, **126**, 13736; (*g*) H. Liu, Z. Lv, K. Ding, X. Liu, L. Yuan, H. Chen and X. Li, *J. Mater. Chem. B*, 2013, **1**, 5550.
7 X. Gu, J. Yao, G. Zhang and D. Zhang, *Small*, 2012, **8**, 3406.
8 P. Galer, R. C. Korošec, M. Vidmar and B. Šket, *J. Am. Chem. Soc.*, 2014, **136**, 7383.
9 G. Yu, G. Tang and F. Huang, *J. Mater. Chem. C*, 2014, **2**, 6609.
10 C. Shi, Z. Guo, Y. Yan, S. Zhu, Y. Xie, Y. S. Zhao, W. Zhu and H. Tian, *ACS Appl. Mater. Interfaces*, 2013, **5**, 192.
11 (*a*) J. Wang, J. Mei, R. Hu, J. Z. Sun, A. Qin and B. Z. Tang, *J. Am. Chem. Soc.*, 2012, **134**, 9956; (*b*) R. Hu, J. W. Y. Lam, H. Deng, Z. Song, C. Zheng and B. Z. Tang, *J. Mater. Chem. C*, 2014, **2**, 6326; (*c*) E. Wang, J. W. Y. Lam, R. Hu, C. Zhang, Y. S. Zhao and B. Z. Tang, *J. Mater. Chem. C*, 2014, **2**, 1801.
12 (*a*) J. C. Y. Ng, H. Li, Q. Yuan, J. Liu, C. Liu, X. Fan, B. S. Li and B. Z. Tang, *J. Mater. Chem. C*, 2014, **2**, 4615; (*b*) H. Li, J. Cheng, Y. Zhao, J. W. Y. Lam, K. S. Wong, H. Wu, B. S. Li and B. Z. Tang, *Mater. Horiz.*, 2014, **1**, 518.
13 B. S. Li, K. K. L. Cheuk, D. Yang, J. W. Y. Lam, L. J. Wan, C. Bai and B. Z. Tang, *Macromolecules*, 2003, **36**, 5447.
14 (*a*) E. T. Chernick, G. Börzsönyi, C. Steiner, M. Ammon, D. Gessner, S. Frühbeißer, F. Gröhn, S. Maier and R. R. Tykwinski, *Angew. Chem., Int. Ed.*, 2014, **53**, 310; (*b*) P. K. Sukul, P. K. Singh, S. K. Maji and S. Malik, *J. Mater. Chem. B*, 2013, **1**, 153.
15 J. Liu, H. Su, L. Meng, Y. Zhao, C. Deng, J. C. Y. Ng, P. Lu, M. Faisal, J. W. Y. Lam, X. Huang, H. Wu, K. S. Wong and B. Z. Tang, *Chem. Sci.*, 2012, **3**, 2737.
16 K. K. L. Cheuk, J. W. Y. Lam, J. Chen, L. M. Lai and B. Z. Tang, *Macromolecules*, 2003, **36**, 5947.
17 (*a*) H. Maeda, Y. Bando, K. Shimomura, I. Yamada, M. Naito, K. Nobusawa, H. Tsumatori and T. Kawai, *J. Am. Chem. Soc.*, 2011, **133**, 9266; (*b*) J. Yuasa, T. Ohno, H. Tsumatori, R. Shiba, H. Kamikubo, M. Kataoka, Y. Hasegawa and

T. Kawai, *Chem. Commun.*, 2013, 4604; (*c*) C. Wagenknecht, C.-M. Li, A. Reingruber, X.-H. Bao, A. Goebel, Y.-A. Chen, Q. Zhang, K. Chen and J.-W. Pan, *Nat. Photonics*, 2010, **4**, 549; (*d*) J. C. Y. Ng, J. Liu, H. Su, Y. Hong, H. Li, J. W. Y. Lam, K. S. Wong and B. Z. Tang, *J. Mater. Chem. C*, 2014, **2**, 78.

18 (*a*) K. Nakamura, S. Furumi, M. Takeuchi, T. Shibuya and K. Tanaka, *J. Am. Chem. Soc.*, 2014, **136**, 5555; (*b*) Y. Morisaki, M. Gon, T. Sasamori, N. Tokitoh and Y. Chujo, *J. Am. Chem. Soc.*, 2014, **136**, 3350; (*c*) E. M. Sánchez-Carnerero, F. Moreno, B. Maroto, A. R. Agarrabeitia, M. J. Ortiz, B. G. Vo, G. Muller and S. de la Moya, *J. Am. Chem. Soc.*, 2014, **136**, 3346; (*d*) K. Okano, M. Taguchi, M. Fujiki and T. Yamashita, *Angew. Chem., Int. Ed.*, 2011, **50**, 12474; (*e*) T. Kaseyama, S. Furumi, X. Zhang, K. Tanaka and M. Takeuchi, *Angew. Chem., Int. Ed.*, 2011, **50**, 3684.

19 (*a*) Y. Kitayama, T. Amako, N. Suzuki, M. Fujiki and Y. Imai, *Org. Biomol. Chem.*, 2014, **12**, 4342; (*b*) H. Oyama, K. Nakano, T. Harada, R. Kuroda, M. Naito, K. Nobusawa and K. Nozaki, *Org. Lett.*, 2013, **15**, 2104; (*c*) T. Amako, T. Kimoto, N. Tajima, M. Fujiki and Y. Imai, *RSC Adv.*, 2013, **3**, 6939; (*d*) H. Maeda, Y. Bando, K. Shimomura, I. Yamada, M. Naito, K. Nobusawa, H. Tsumatori and T. Kawai, *J. Am. Chem. Soc.*, 2011, **133**, 9266.

20 (*a*) H. v. Berlepsch, K. Ludwig, B. Schade, R. Haag and C. Böttcher, *Adv. Colloid Interface Sci.*, 2014, **208**, 279; (*b*) H. Lu, J. Wang, Z. Song, L. Yin, Y. Zhang, H. Tang, C. Tu, Y. Lin and J. Cheng, *Chem. Commun.*, 2014, 139; (*c*) S. Datta, S. K. Samanta and S. Bhattacharya, *Chem.–Eur. J.*, 2013, **19**, 11364; (*d*) H. Cao, Q. Yuan, X. Zhu, Y.-P. Zhao and M. Liu, *Langmuir*, 2012, **28**, 15410.

21 H. Shi, R. T. Kwok, J. Liu, B. Xing, B. Z. Tang and B. Liu, *J. Am. Chem. Soc.*, 2012, **134**, 17972.

